

Self-induced back-action optical trapping of dielectric nanoparticles

Mathieu L. Juan^{1*}, Reuven Gordon^{1,2*}, Yuanjie Pang², Fatima Eftekhari² and Romain Quidant^{1,3†}

Optical trapping has widely affected both the physical and life sciences. Past approaches to optical trapping of nanoscale objects required large optical intensities, often above their damage threshold. To achieve more than an order of magnitude reduction in the local intensity required for optical trapping, we present a self-induced back-action (SIBA) optical trap, where the trapped object has an active role in enhancing the restoring force. We demonstrate experimentally trapping of a single 50 nm polystyrene sphere using a SIBA optical trap on the basis of the transmission resonance of a nanoaperture in a metal film. SIBA optical trapping shows a striking departure from previous approaches, which we quantify by comprehensive calculations. The SIBA optical trap enables new opportunities for non-invasive immobilization of a single nanoscale object, such as a virus or a quantum dot.

Optical trapping has found many applications in the physical and life sciences because it allows for precise control and positioning of micrometre-sized dielectric objects^{1,2}. For example, optical trapping has been applied to objects of biological interest, such as cells, bacteria and viruses, to indirectly manipulate DNA and to measure the forces involved in RNA transcription^{3,4}. There are two fundamental challenges in extending optical trapping to nanoscale objects, smaller than 100 nm, with a refractive index close to, but greater than, the surrounding medium. First, the gradient optical force becomes much weaker as the object gets smaller, scaling with the third power of its size. Second, the thermal motion of the object increases with decreasing object size owing to a reduction in the viscous drag, thereby favouring escape from the trap. So far, the only approach to trap smaller objects is to increase the trapping laser intensity; halving the particle size requires an order of magnitude increase in the local field intensity within the trap. Consequently, trapping very small objects involves intensities that can exceed their damage threshold. For example, a previous work reported that 109-nm-diameter polystyrene particles survived only 25 s in a focused beam optical trap, and 85-nm particles were damaged so quickly that they could not be measured reliably¹. Optical damage becomes even more important for biological specimens^{3,5}, where small thermal changes are critical.

An alternative to conventional lens-based optical tweezers uses nanostructures to focus light below the diffraction limit and enhance the local optical intensity within the trap^{6–9}. As a result, the nanostructure can increase the potential energy and the confinement of the trap^{10–12}. Nanoscale objects have been confined to subwavelength regions using nanostructured optical traps^{13–16}. For example, a recent work has shown one-dimensional trapping of 76-nm dielectric particles in the vicinity of a Si slot waveguide coupled to a 300 mW laser beam¹³. For those past approaches to trapping with nanostructures, the trapping followed the usual perturbative Rayleigh gradient force, so photo damage remains a concern. Evanescent whispering-gallery modes in microsphere resonators have also been used to trap and sense nanoparticles and viruses; however, in that configuration the particle moves around

the circumference of the microsphere without being confined in three dimensions^{17,18}.

Here, we consider the possibility of creating an optical trap in which the particle itself has a strong influence on the local electric field and thereby has an active role in the trapping mechanism. This so-called self-induced back-action (SIBA) optical trapping is enhanced by the use of an optical resonance. Our approach differs in a fundamental way from trapping using resonances of atoms^{19,20} or quantum dots²¹: here, there is no resonance required from the trapped object; it is only a generic dielectric particle and the resonance is sustained by the trap itself. In this work, we demonstrate a SIBA optical trap using a nanoaperture in a metal film that is close to its cutoff resonance²². The SIBA mechanism provides superior trapping ability for Rayleigh particles, with improved performance as the particle size is reduced. It is important to emphasize that in this situation the aperture is only a model system; SIBA could be implemented in other systems where the presence of the trapping object enhances the local electric field. Our experiments show the trapping of 100-nm and 50-nm polystyrene spheres, with incident powers of only 0.7 mW and 1.9 mW, respectively. Beyond substantially decreasing the minimum incident laser intensity as compared with past approaches, SIBA enables reducing by one order of magnitude the local intensity within the trap.

The experiment used a 310-nm-diameter cylindrical aperture made by focused-ion-beam milling in a 100-nm-thick gold film on a glass substrate, as shown schematically in Fig. 1. (Further details are provided in the Supplementary Information.) This aperture–film sample was inserted into a liquid chamber containing 0.05% w/v spherical polystyrene particles (refractive index of 1.575) of either 100 nm or 50 nm diameter in water (refractive index of 1.33) with a 5% concentration of sodium dodecyl sulphate solution (5% w/v) to prevent aggregation. The sample was mounted upside-down so that gravity pulls the particles away from the gold film. The light from a 1,064 nm wavelength continuous-wave Nd:YAG laser was focused onto the aperture using a $\times 40$ microscope objective (0.65 numerical aperture) to a 2- μm -diameter spot-size. The illumination was linearly polarized along the X direction. Under this polarization, stable trapping occurs at the aperture side on the

¹IICFO-Institut de Ciències Fotoniques, Mediterranean Technology Park, 08860 Castelldefels, (Barcelona), Spain, ²Department of Electrical and Computer Engineering, University of Victoria, Victoria, British Columbia, V8W 3P6, Canada, ³ICREA-Institut de Recerca i Estudis Avançats, Barcelona, 08010, Spain. *These authors contributed equally to this work. †e-mail: romain.quidant@icfo.es.

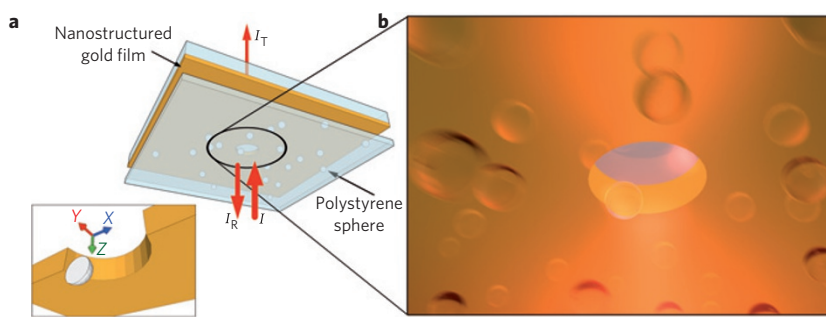


Figure 1 | SIBA optical trapping using a nanoaperture in a metallic film. **a**, Schematic representation of the trapping set-up for a 310 nm aperture in a 100-nm-thick gold film and 100-nm polystyrene spheres in water. The diagram in the left-bottom corner shows the coordinate system used, with the origin at the centre of the aperture. **b**, Schematic of the trapping of a single polystyrene sphere, while others experience thermal diffusion.

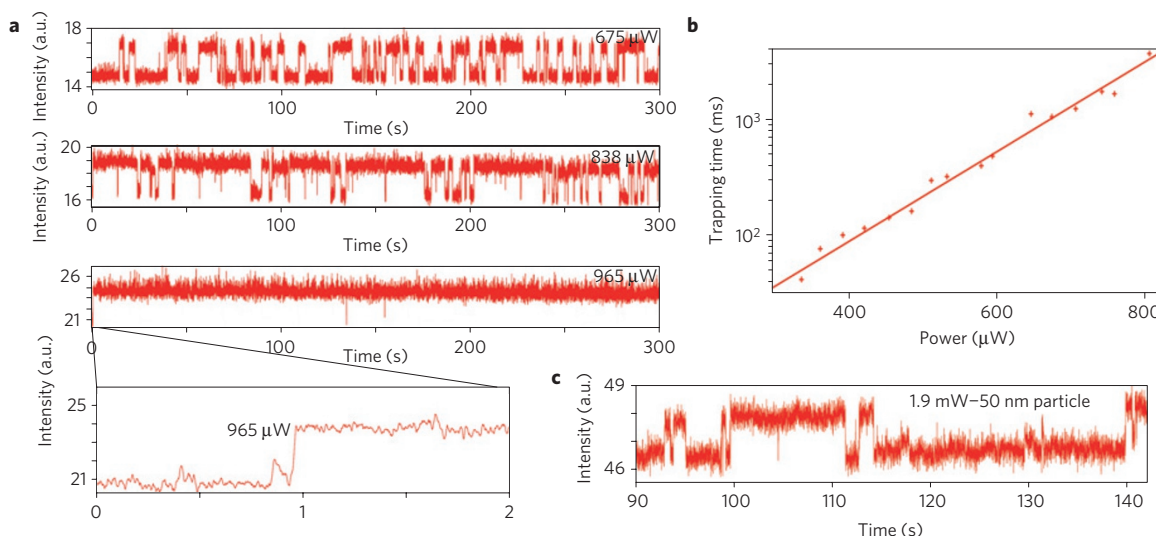


Figure 2 | Experimental trapping of 100- and 50-nm particles. **a**, Experimental time evolution of the intensity transmitted through a 310 nm aperture using different incident laser power when exposed to a solution of 100-nm polystyrene particles. Abrupt increases are from a particle trapped in the aperture. **b**, Evolution of the trapping time as a function of the incident power. The crosses are the experimental data; the line is the exponential fit corresponding to the Arrhenius law. **c**, Experimental time evolution of the transmitted intensity showing the trapping of a 50 nm particle at 1.9 mW.

X axis. The aperture was chosen to have a calculated transmission cutoff resonance in solution of 990 nm, just shorter than the laser wavelength of 1,064 nm (refs 23–25). A schematic diagram of the experimental geometry is shown in Fig. 1a, where I , I_R and I_T are the incident, reflected and transmitted intensities, respectively. As the aperture's transmission resonance is sensitive to small changes of the local refraction index, the presence of a particle in the aperture can be tracked by changes in the transmitted and reflected intensities. Figure 1b shows a schematic of a 100 nm polystyrene bead particle trapped at the aperture.

Above the cutoff resonance of the aperture, the optical transmission is particularly sensitive to the location of the particle owing to the associated change of its surrounding refractive index. Having a larger refractive index than water, a particle occupying the aperture makes the aperture 'appear' larger, which allows for more transmission above the usual cutoff wavelength. To illustrate the SIBA effect, we consider the equilibrium point for the particle at the opening of the aperture on the side of optical incidence, the forces associated with the change in photon transmission rate, and Newton's third law. The transmission drops when the particle is moved away from the aperture, with a corresponding drop in the rate of photon momentum travelling through the aperture. By Newton's third law, it is expected that a force in the opposite direction will act on the particle to balance this momentum rate change; the balancing force will be directed towards the aperture,

thereby pulling the particle back to the equilibrium position. On the other hand, if the particle moves further into the aperture the transmission will increase and the restoring force will push the particle out. There is also a lateral force that arises from the symmetry breaking of an offset particle in the aperture. As the particle moves towards the edge, it concentrates the field there to enhance the trapping. This is most evident from the calculations that show the redistribution of the local field from the particle (see Supplementary Information). In this way, the SIBA effect provides an extra physical mechanism, in addition to the conventional gradient force, which enhances the trapping efficiency.

The observed time evolution of the nanoaperture transmission resulting from trapping of 100-nm particles is shown in Fig. 2a, for incident powers of 675, 838 and 965 μ W. We applied a seven-point-window second-order Savitzky–Golay algorithm to smooth out the noise from 2.5 ms fast sampling. During laser exposure, the transmission showed abrupt jumps, revealing two discrete states. Moreover, the occurrence and duration of these states depended strongly on the incident power. No corresponding changes in the transmitted intensity were observed for a solution without particles. Owing to gravity, the particles were pulled away from the aperture when the laser was off. The recording of the transmitted intensity began immediately after the laser was turned on. Therefore, the initial lower intensity values of the transmission were thus obtained in the absence of particles in the aperture. By turning on the laser,

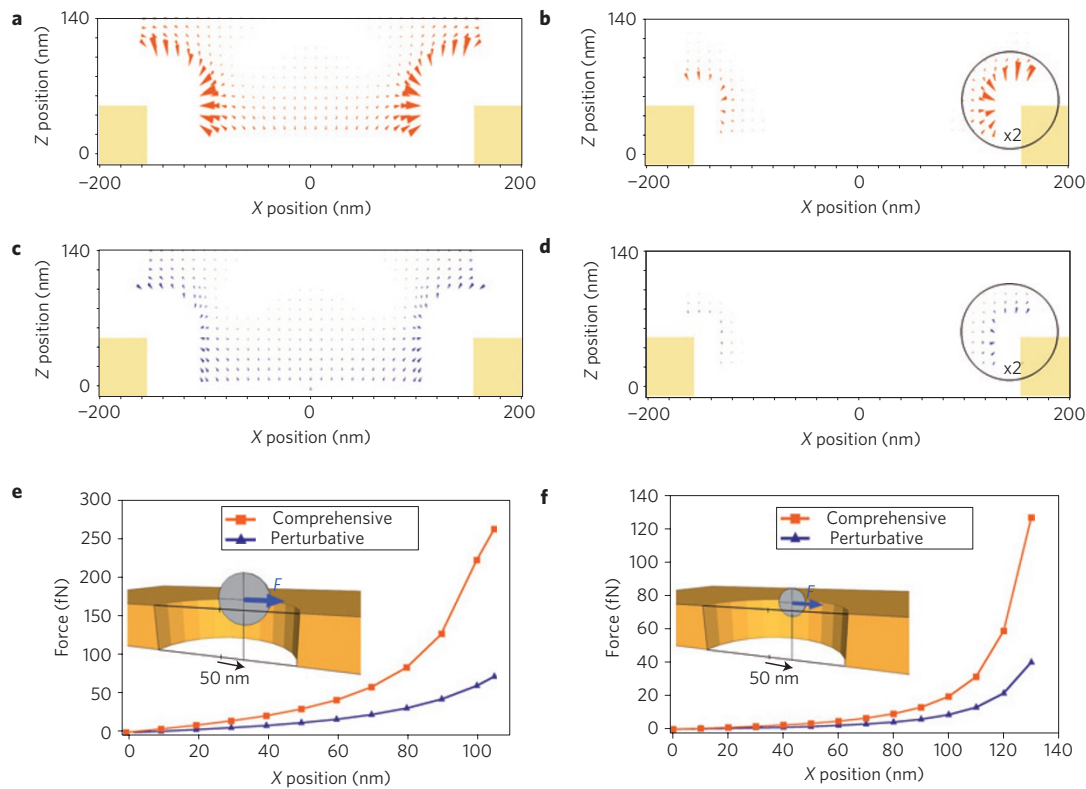


Figure 3 | Numerical evaluation of SIBA trapping. **a-d**, Numerical force field calculated for 100-nm particles (**a,c**) and for 50-nm particles (**b,d**) using a comprehensive MST analysis of FDTD calculations (**a,b**) and a perturbative method based on gradient forces (**c,d**). The insets in **b** and **d** show two times force magnifications. **e,f**, The lateral trapping force acting on 100-nm (**e**) and 50-nm particles (**f**) as a function of the distance to the aperture centre obtained with the comprehensive and the perturbative method. The calculations were made for an injected power in the aperture of 1 mW.

the optical scattering force gently agitated the particles. It should be noted that the optical scattering force was five orders of magnitude smaller than the gradient force, so that it had no role in the observed trapping (see Supplementary Information).

The time evolution of the transmission, presented in Fig. 2a, shows clearly the trapping of a single 100 nm polystyrene particle, where the higher value of the transmission corresponds to the time when a particle occupied the aperture. Stable trapping over an acquisition time of 5 min was observed for a relatively small incident power of 1 mW, corresponding to a maximum intensity in the focus centre of $1 \text{ mW } \mu\text{m}^{-2}$. This is an improvement over powers larger than 12 mW, as found for a conventional trap for 109-nm polystyrene spheres¹. Accounting for the higher numerical aperture and the wavelength used in that work, the maximum intensity is estimated to have been $110 \text{ mW } \mu\text{m}^{-2}$, two orders of magnitude larger than in our experiment.

Figure 2b shows the dependence of the trapping time τ on the incident power. It shows clearly the exponential behaviour expected from the Arrhenius law, where the incident power is linearly related to the trapping potential: $\tau = A \exp(U_{\text{trap}}/kT)$, with U_{trap} being the trapping potential, A a constant and kT the thermal energy, where k is the Boltzmann constant and T is the temperature. The variance in trapping time was found to be close to the mean value for all power levels. The trapping time distribution fits well to an exponential distribution, which is consistent with the Poisson statistics characteristic of independent events (see Supplementary Information).

To obtain further insight into the SIBA trapping mechanism, we carried out a numerical evaluation of the active role of the trapped specimen. Usually, the trapping force experienced by low-refractive-index nanoscale objects in the Rayleigh regime is calculated with a perturbative approach. In the perturbative

approach, first the electromagnetic fields are computed without the object and then the gradient and scattering forces on the particle are calculated using the point-dipole approximation²⁶. Several works have included the particle in the electromagnetic simulations *a priori*, and then used the Maxwell stress tensor (MST) method to calculate the trapping forces²⁷. Usually, the comprehensive MST calculations and the perturbative dipole approximation agree well for particles in the Rayleigh regime²⁸. Close agreement between the two approaches, to within approximately 10%, has even been shown for recent works on nanostructured optical traps²⁹. For our calculations, however, there is a large discrepancy between the two approaches and the perturbative approach is no longer valid. This discrepancy arises precisely because the SIBA optical trap is not perturbative: the particle itself has an active and favourable role in the trapping.

The force field in the vertical plane was calculated using both the perturbative approach and the comprehensive MST calculation, as shown in Fig. 3. The potential well was found to be nearly isotropic in this plane. We found that the MST approach (Fig. 3a,b) gives substantially greater force magnitudes over the perturbative approach (Fig. 3c,d).

To quantify the active role of the particle in the trapping mechanism, we computed the incident light intensity required to obtain a trapping energy equal to the thermal energy ($kT = 4.0 \times 10^{-21} \text{ J}$). For the 100-nm particles, the required incident intensity is $250 \mu\text{W } \mu\text{m}^{-2}$ for the MST as compared with $870 \mu\text{W } \mu\text{m}^{-2}$ for the perturbative case. For a 50 nm particle, the influence of the particle was found to be even greater, with required intensities of 1.6 and $20 \text{ mW } \mu\text{m}^{-2}$ for the MST and perturbative cases, respectively. In other words, the active role of the 50 nm particle in the trapping efficiency reduces the incident intensity requirement by an order of magnitude as compared with the perturbative approach.

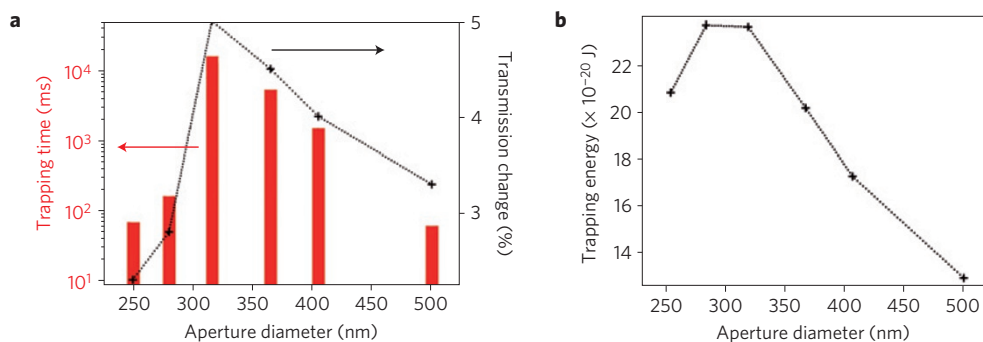


Figure 4 | Trapping time evolution with the aperture diameter for 100 nm particles at 1.6 mW. **a**, Experimental evolution of the average trapping time with the aperture diameter (red bars). In addition, the changes in the transmitted intensity related to the trapping of a particle are presented (black curve). **b**, Theoretical evolution of the trapping energy with the aperture diameter.

In the SIBA trap, the trapping stiffness calculation is also strongly modified when using the full MST calculation as compared with the commonly used perturbative method (Fig. 3e,f). Using the MST approach, we obtained a theoretical stiffness for 1 W of injected power of 9.3 pN nm^{-1} and 6.6 pN nm^{-1} for the 100- and 50-nm particles respectively at the minimum energy trapping point at the side of the hole and along the X direction. The stiffness on the Z direction is similar, with 8.2 pN nm^{-1} and 7.2 pN nm^{-1} (see Supplementary Information). For comparison, a previous work reported a 0.2 pN nm^{-1} for 100-nm particles¹³.

To show the influence of the aperture resonance on the SIBA, we considered tuning the resonance properties by adjusting the aperture size. Figure 4 shows both experiment and theory for various aperture sizes at a constant incident power of 1.6 mW. The trapping time is maximized for aperture sizes close to the cutoff, as shown in Fig. 4a. Compared with the 500 nm aperture, which is the same size as used in a previous work¹⁵, the trapping time of a 316 nm aperture is increased by over two orders of magnitude. The percentage change in the measured transmitted intensity is doubled for the 316 nm aperture, showing a stronger feedback effect from the photon momentum change in the aperture close to its cutoff. The trapping energy was also calculated for different aperture sizes, and it was found to double when increasing the aperture size from 310 to 500 nm. Therefore, both experimental and theoretical data show clearly a maximized SIBA effect close to the cutoff resonance of the aperture.

Past works relied on a strong enhancement of the local intensity provided by the nanostructure. Here, the local intensity is only moderately enhanced by the nanostructure, by a factor of seven. This is one of the main benefits of the SIBA trap: efficient trapping can be achieved with factor of 20 lower local intensities than found previously¹³ when accounting for the local enhancement of the trapping structure, thereby drastically reducing the likelihood of optical damage.

Exploiting SIBA optical trapping, we were also able to trap experimentally 50-nm polystyrene spheres. Figure 2c shows the time evolution of the transmission through the 310 nm aperture with an incident laser power of only 1.9 mW.

We have demonstrated SIBA optical trapping capable of stabilizing 50-nm nanoparticles, within a subwavelength volume, with less than 2 mW of total power. The active role of the particle in the optical trap allowed for an order-of-magnitude improved trapping efficiency over the usual perturbative approach, as confirmed by both experimental results and comprehensive numerical simulations. Such enhanced performance comes along with a large decrease, by at least an order of magnitude, of the local intensity experienced by the trapped particle. Low-intensity optical trapping of small dielectric particles ($\sim 50 \text{ nm}$) enables new opportunities for isolating and studying biological nanoscopic

entities, such as viruses. Another interesting feature of our experiment is the possibility to monitor a single trapped nanoscale object through transmission changes. This dual trapping–sensing capability may be useful in sorting applications. In the past, optical trapping configurations have been modified to be sensors for particles that are too small to be trapped, such as viruses³⁰. Here, the proposed approach makes it possible to simultaneously immobilize and sense them in a single nanoscale aperture, providing optical integrated capabilities for biological analysis *in situ*.

Received 12 May 2009; accepted 1 September 2009; published online 11 October 2009

References

1. Ashkin, A., Dziedzic, J. M., Bjorkholm, J. E. & Chu, S. Observation of a single-beam gradient force optical trap for dielectric particles. *Opt. Lett.* **11**, 288–290 (1986).
2. Dholakia, K., Reece, P. & Gu, M. Optical micromanipulation. *Chem. Soc. Rev.* **37**, 42–55 (2008).
3. Ashkin, A. & Dziedzic, J. M. Optical trapping and manipulation of viruses and bacteria. *Science* **235**, 1517–1520 (1987).
4. Yin, H. *et al.* Transcribing against an applied force. *Science* **270**, 1653–1657 (1995).
5. Liu, Y., Sonek, G. J., Berns, M. W. & Tromberg, B. J. Physiological monitoring of optically trapped cells: Assessing the effects of confinement by 1,064 nm laser tweezers using microfluorometry. *Biophys. J.* **71**, 2158–2167 (1996).
6. Huang, L. & Martin, O. J. F. Reversal of the optical force in a plasmonic trap. *Opt. Lett.* **33**, 3001–3003 (2008).
7. Nieto-Vesperinas, M., Chaumet, P. C. & Rahmani, A. Near-field photonic forces. *Phil. Trans. Math. Phys. Eng. Sci.* **362**, 719–737 (2004).
8. Okamoto, K. & Kawata, S. Radiation force exerted on subwavelength particles near a nanoaperture. *Phys. Rev. Lett.* **83**, 4534–4537 (1999).
9. Novotny, L., Bian, R. X. & Xie, X. S. Theory of nanometric optical tweezers. *Phys. Rev. Lett.* **79**, 645–648 (1997).
10. Quidant, R., Petrov, D. & Badenes, G. Radiation forces on a Rayleigh dielectric sphere in patterned optical near field. *Opt. Lett.* **30**, 1009–1011 (2005).
11. Righini, M., Girard, C. & Quidant, R. Light-induced manipulation with surface plasmons. *J. Opt. A: Pure Appl. Opt.* **10**, 093001 (2008).
12. Sainidou, R. & García de Abajo, F. J. Optically tunable surfaces with trapped particles in microcavities. *Phys. Rev. Lett.* **101**, 136802 (2008).
13. Yang, A. H. J. *et al.* Optical manipulation of nanoparticles and biomolecules in sub-wavelength slot waveguides. *Nature* **457**, 71–75 (2009).
14. Righini, M. *et al.* Nano-optical trapping of Rayleigh particles and *Escherichia coli* bacteria with resonant optical antennas. *Nano Lett.* doi:10.1021/nl803677x (2009).
15. Kwak, E. S. *et al.* Optical trapping with integrated near-field apertures. *J. Phys. Chem. B* **108**, 13607–13612 (2004).
16. Grigorenko, A. N., Roberts, N. W., Dickinson, M. R. & Zhang, Y. Nanometric optical tweezers based on nanostructured substrates. *Nature Photon.* **2**, 365–370 (2008).
17. Arnold, S. *et al.* Whispering gallery mode carousel—a photonic mechanism for enhanced nanoparticle detection in biosensing. *Opt. Express* **17**, 6230–6238 (2009).
18. Vollmer, F., Arnold, S. & Keng, D. Single virus detection from the reactive shift of a whispering-gallery mode. *Proc. Natl Acad. Sci. USA* **105**, 20701–20704 (2008).
19. Adams, C. S. & Riis, E. Laser cooling and trapping of neutral atoms. *Prog. Quant. Electron.* **21**, 1–79 (1997).

20. Pinkse, P. W. H., Fisher, T., Maunz, P. & Rempe, G. Trapping an atom with single photons. *Nature* **404**, 365–368 (2000).
21. Iida, T. & Ishihara, H. Theoretical study of the optical manipulation of semiconductor nanoparticles under excitonic resonance condition. *Phys. Rev. Lett.* **90**, 057403 (2003).
22. Genet, C. & Ebbesen, T. W. Light in tiny holes. *Nature* **445**, 39–46 (2007).
23. García-Vidal, F. J., Moreno, E., Porto, J. A. & Martín-Moreno, L. Transmission of light through a single rectangular hole. *Phys. Rev. Lett.* **95**, 103901 (2005).
24. García-Vidal, F. J., Martín-Moreno, L., Moreno, E., Kumar, L. K. S. & Gordon, R. Transmission of light through a single rectangular hole in real metal. *Phys. Rev. B* **74**, 153411 (2006).
25. García de Abajo, F. Light transmission through a single cylindrical hole in a metallic film. *Opt. Express* **10**, 1475–1484 (2002).
26. Neuman, K. C. & Block, S. M. Optical trapping. *Rev. Sci. Instrum.* **75**, 2787–2809 (2004).
27. Chaumet, P. C., Rahmani, A. & Nieto-Vesperinas, M. Optical trapping and manipulation of nano-objects with an apertureless probe. *Phys. Rev. Lett.* **88**, 123601 (2002).
28. Rohrbach, A. & Stelzer, E. H. K. Optical trapping of dielectric particles in arbitrary fields. *J. Opt. Soc. Am. A* **18**, 839–853 (2001).
29. Yang, A. H. J., Lerdsuchawanich, T. & Erickson, D. Forces and transport velocities for a particle in a slot waveguide. *Nano Lett.* **9**, 1182–1188 (2009).
30. Ignatovich, F. V., Topham, D. & Novotny, L. Optical detection of single particles and viruses. *IEEE J. Sel. Top. Quant. Electron.* **12**, 1292–1300 (2006).

Acknowledgements

This work was supported by the Spanish Ministry of Sciences through Grants TEC2007-60186/MIC and CSD2007-046-NanoLight.es and Fundació CELLEX Barcelona. R.G., Y.P. and F.E. supported by the Natural Sciences and Engineering Research Council (NSERC) of Canada Discovery Grant. R.G. was supported for this work through a visiting professorship from the Agència de Gestió d'Ajuts Universitaris i de Recerca (AGAUR) Generalitat de Catalunya.

Author contributions

M.L.J., R.G. and R.Q. planned the project, designed the experiment and wrote the paper. M.L.J. did the trapping experiments on samples prepared by F.E. Y.P. and R.G. carried out the numerical simulations. All of the authors participated in the analysis of the results.

Additional information

Supplementary information accompanies this paper on www.nature.com/naturephysics. Reprints and permissions information is available online at <http://npg.nature.com/reprintsandpermissions>. Correspondence and requests for materials should be addressed to R.Q.